

Terahertz emission from ultrafast optical orientation of spins in semiconductors: Experiment and theory

F. Nastos, R. W. Newson, J. Hübner,* H. M. van Driel, and J. E. Sipe

Department of Physics and Institute for Optical Sciences, University of Toronto, 60 Street George Street, Toronto, Ontario, Canada M5S 1A7

(Received 3 March 2008; published 6 May 2008)

We discuss the optical injection of magnetization into a nonmagnetic semiconductor by the absorption of circularly polarized light. A microscopic approach, which is based on Fermi's golden rule and $\mathbf{k}\cdot\mathbf{p}$ band models, is used to quantify the magnetization-injection rate in GaAs. We find that under conditions typical in optical orientation experiments, the magnetization-injection rate of holes is approximately 20 times larger than it is for electrons, reflecting the large hole magnetic moment. We then turn to the ultrafast excitation regime and explore the possibility that the injected magnetization can radiate a detectable terahertz field. By using a phenomenological approach for the magnetization relaxation dynamics, we predict that the terahertz field from magnetic injection is at the limit of current terahertz detection technology. We provide initial experimental measurements in search of this terahertz radiation.

DOI: [10.1103/PhysRevB.77.195202](https://doi.org/10.1103/PhysRevB.77.195202)

PACS number(s): 72.25.Fe

I. INTRODUCTION

A host of recent fundamental studies on the behavior of spins in semiconductors has been motivated by the idea of using the spin degree of freedom in information processing, which is the goal of a field that has come to be known as *spintronics*. Central to many of these investigations has been the optical injection of spin polarized electrons and holes in semiconductors, which is a process that is called *optical orientation*.^{1,2} These spin polarized carriers are then available to be dragged by a bias voltage, for example, to regions of interest in any proposed device structure. Common techniques for measuring the optical orientation do so by monitoring, after excitation, the populations in various bands or their effect on luminescence or Faraday rotation.^{3,4} In such studies, the spins of the holes are usually neglected. This is because the electron-spin lifetime is much longer than the hole spin lifetime, which is commonly assumed to be shorter than any other time scales of interest. However, recent ultrafast pump-probe experiments by Hilton and Tang⁵ measured the heavy-hole spin lifetime to be 110 fs, which indicates the possibility that hole dynamics may play an important role in at least some ultrafast experiments.

Especially if the dynamics of both electrons and holes are to be considered, it can be argued that the magnetic moments of these carriers deserve more attention than they have received. Indeed, it has been known for a long time that the holes in a semiconductor can have much larger magnetic moments than the electrons,⁶ and so the holes will make a larger contribution than the electrons to the optical injection of magnetization that accompanies optical orientation. The injection and the subsequent evolution of this magnetization are interesting topics in their own right. With respect to any device applications, designs utilizing spin polarized carriers will, of course, typically involve carriers with a net magnetic moment. Moreover, since both the expectation value of the spin and the magnetic moment can be defined for a Bloch electron,⁷ studies of populations in bands can be taken to reveal the evolution of the magnetic moments of the carriers

just as well as the evolution of their spins. Yet, the magnetic moments of the carriers are arguably more directly measurable than their spins.

In this paper, we investigate the magnetic properties of carriers that can be optically injected in bulk GaAs by using circularly polarized light and consider the possibility that the transient magnetization can be detectable via the emitted terahertz radiation. The observation of such a signal would constitute a direct observation of the ultrafast magnetization of GaAs by the optical injection of carriers, in contrast to the more indirect measurements that follow from pump-probe or luminescence experiments detecting band populations. Moreover, since the holes make a much larger contribution to the injected magnetization than the electrons, the study of the injection and decay of magnetization by its terahertz radiation could provide an important window to the dynamics of optically injected holes in semiconductors.

The optical injection of magnetization we focus on here is phenomenologically similar to the inverse Faraday effect (IFE).⁸⁻¹⁰ Previous works on the IFE have largely focused on optically induced magnetization in the nonabsorbing regime^{8,9} or in metallic systems.¹¹ Popov *et al.*¹² considered the specular reflection from the IFE, in both the absorbing and the nonabsorbing cases, and measured the effective χ_3 nonlinearity describing the reflection, but they did not focus on the microscopic description of the effect. When pumping with circularly polarized light, the effect on the probe beam polarization can come from an injected magnetization or from the Pauli blocking.¹³⁻¹⁵

The outline of the paper is as follows: In Sec. II A, we discuss the optical injection of magnetization in semiconductors, which relates it to the optical injection of carriers and spins. By using model calculations, we study how the magnetic moments of the injected carriers vary as a function of the energy of the photon responsible for the injection. In Sec. II B, we consider the terahertz radiation from the injected magnetization, which is in contrast to the terahertz radiation from the injected (electric-dipole) polarization that also occurs in zinc-blende semiconductors above the band gap, and

show how the polarization of the incident light can be used to distinguish between the two and thus measure one with respect to the other. Estimates of the sizes of the two effects are given, and we show that the electric field strength of the terahertz radiation from the injected magnetization is large enough to be detected by common terahertz detection schemes. In Sec. III, we present the results of initial experiments aimed at detecting this injected magnetization, and in Sec. IV, we conclude.

II. THEORY

A. Optical injection of magnetization

When a semiconductor is excited by photons with energies above the band gap, electrons and holes are injected at a rate \dot{n} that closely follows in time the laser intensity pulse profile in the sample. The carrier density injection rate \dot{n} is given by

$$\dot{n}(\mathbf{r}, t) = \xi^{ab}(\omega_0) E_{\text{env}}^{a*}(\mathbf{r}, t) E_{\text{env}}^b(\mathbf{r}, t) + \text{c.c.} \quad (1)$$

The italic superscripts indicate the Cartesian coordinates that are to be summed over when repeated, $\xi^{ab}(\omega_0)$ is proportional to the absorption coefficient evaluated at a carrier frequency ω_0 , and $E_{\text{env}}^a(\mathbf{r}, t)$ is the temporal envelope function of the laser electric field profile $E^a(\mathbf{r}, t)$, which is given by

$$E^a(\mathbf{r}, t) = E_{\text{env}}^a(\mathbf{r}, t) e^{-i\omega_0 t} + \text{c.c.} \quad (2)$$

We have assumed, as is commonly done, that the absorption coefficient does not vary much over the spectral width of the laser pulse. From the form given by Eq. (1), the temporal behavior of $\dot{n}(\mathbf{r}, t)$ is solely determined by the laser pulse envelope.

From a microscopic perspective, the injection rate \dot{n} can be calculated from Fermi's golden rule, which gives the well-known result that¹⁶

$$\xi^{ab}(\omega) = \frac{2\pi e^2}{\hbar^2} \sum_{c,v} \int \frac{d^3k}{8\pi^3} r_{vc}^a(\mathbf{k}) r_{cv}^b(\mathbf{k}) \delta[\omega_{cv}(\mathbf{k}) - \omega], \quad (3)$$

where $r_{cv}^a(\mathbf{k})$ is the dipole matrix element between bands c and v at a point \mathbf{k} in the Brillouin zone and $\hbar\omega_c(\mathbf{k})$ is the energy of the Bloch state at \mathbf{k} in band c . In the summation, c is restricted to conduction bands and v to valence bands.

Accompanying the carrier injection can be an injection of current,^{17,18} spin current,¹⁹ (electric-dipole) polarization,^{20,21} spin,^{1,22} or magnetization,¹³ which depends on the polarization of the light source. Optical orientation (spin injection) arises from *circularly* polarized excitation of carriers. For excitation of GaAs, near the band edge, the physics is well known.¹ The highest valence bands are comprised of two heavy bands and two light bands. At Γ , these are all degenerate; the heavy valence bands have a magnetic quantum number $m_{j_v} = \pm \frac{3}{2}$ and the light valence bands have $m_{j_v} = \pm \frac{1}{2}$. The corresponding hole states have magnetic quantum numbers $m_{j_h} = -m_{j_v}$. The two lowest conduction bands at Γ are comprised of a spin-up and a spin-down state ($m_{j_c} = \pm \frac{1}{2}$). These states are depicted in Fig. 1. Excitation with σ^+ polarized photons, with an energy just above the band gap energy,

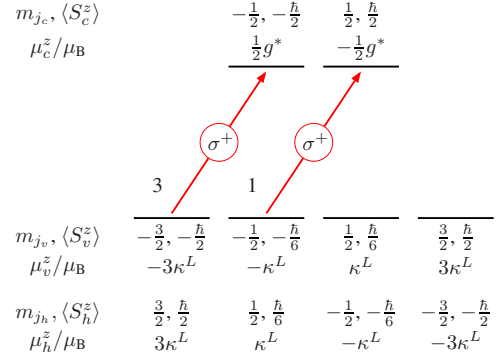


FIG. 1. (Color online) Schematic of the zone center energy levels of the highest valence and lowest conduction states in GaAs. The two conduction states are degenerate as are the four valence states, and the figure denotes the states in the z -quantized basis. The quantities under (over) the valence (conduction) state levels are denoted in the left margin: m_{j_v} is the total magnetic quantum number of the valence state, m_{j_h} of the corresponding hole state, and m_{j_c} of the conduction state. $\langle S^z \rangle$ is the expectation value of the z component of spin, and μ^z / μ_B is the z component of the magnetic moment in units of μ_B . Note that the values for holes are the negative of the valence state values. The two red arrows denote the transitions excited by σ^+ polarized photons of energy equal to the band gap. The numbers (3 and 1) next to the arrows denote the relative strength of the transitions.

excites two transitions: one that creates $m_{j_h} = \frac{3}{2}$ holes and $m_{j_c} = -\frac{1}{2}$ electrons and another that creates $m_{j_h} = \frac{1}{2}$ holes and $m_{j_c} = \frac{1}{2}$ electrons. For each transition, $m_{j_h} + m_{j_c} = 1$, which is associated with the angular momentum from the photon. The relative strengths of these two transitions are 3:1, so that for every four σ^+ photons absorbed, three $m_{j_c} = -\frac{1}{2}$ and one $m_{j_c} = \frac{1}{2}$ electrons are created. This gives a mean electron spin \bar{s}_e equal to $[3(-\frac{\hbar}{2}) + 1(\frac{\hbar}{2})] / (3+1) = -\frac{1}{2}(\frac{\hbar}{2})$, or -50% polarization; thus, the net rate of electron-spin injection is $\dot{S}_e(\mathbf{r}, t) = \bar{s}_e \dot{n}(\mathbf{r}, t)$.

Under excitation of σ^+ light, the injection rate for hole spin density is similarly given by $\dot{S}_h(\mathbf{r}, t) = \bar{s}_h \dot{n}(\mathbf{r}, t)$. The spin of the created heavy-hole states is $\frac{\hbar}{2}$ and that of the light-hole states is $\frac{\hbar}{6}$. The three-to-one weighing gives $\bar{s}_h = [3(\frac{\hbar}{2}) + \frac{\hbar}{6}] / 4$ or $\frac{5}{6}(\frac{\hbar}{2})$. Even though the light does not directly couple to the spin, the spin-orbit interaction leads to a net spin density $S_e + S_h$ being injected.

Since the carriers have a magnetic moment, the net spin imbalance induced by optical orientation suggests a net magnetization. To quantify this magnetization injection, we need the magnetic moments of the carriers. The magnetic moment of a free electron is $\mu = -g\mu_B s / \hbar$, where μ_B is the Bohr magneton, $s = \hbar/2$, and $g = 2.0023$ is the free electron g factor. In a crystal, however, the magnetic moment of an injected carrier includes contributions from both spin and orbital angular momentum. For states $|m\mathbf{k}\rangle$ and $|n\mathbf{k}\rangle$, the matrix element $\mu_{mn}^z(\mathbf{k})$ of the z component of the magnetic moment,

$$\mu_{mn}^z(\mathbf{k}) \delta(\mathbf{k} - \mathbf{k}') = \langle m\mathbf{k} | \hat{\mu}^z | n\mathbf{k}' \rangle, \quad (4)$$

is given by the generalized Roth formula,⁷

$$\mu_{mn}^z(\mathbf{k}) = -\frac{g\mu_B\sigma_{mn}^z(\mathbf{k})}{2} - \frac{1}{mi} \sum_{s \neq m,n} \frac{p_{ms}^x(\mathbf{k})p_{sn}^y(\mathbf{k}) - p_{ms}^y(\mathbf{k})p_{sn}^x(\mathbf{k})}{\epsilon_n(\mathbf{k}) - \epsilon_s(\mathbf{k})}, \quad (5)$$

where p_{ms}^x is the x component of the momentum matrix element between the states $|m\mathbf{k}\rangle$ and $|s\mathbf{k}\rangle$,

$$p_{ms}^x(\mathbf{k})\delta(\mathbf{k} - \mathbf{k}') = \langle m\mathbf{k}|\hat{p}^x|s\mathbf{k}'\rangle, \quad (6)$$

where $\epsilon_s(\mathbf{k})$ is the energy eigenvalue associated with state $|s\mathbf{k}\rangle$ and σ_{mn}^z is the matrix element of the Pauli spin operator $\hat{\sigma}^z$,

$$\sigma_{mn}^z(\mathbf{k})\delta(\mathbf{k} - \mathbf{k}') = \langle m\mathbf{k}|\hat{\sigma}^z|n\mathbf{k}'\rangle. \quad (7)$$

The magnetic moment of the electrons is often expressed relative to the spin state by $\mu_e = -g^*\mu_B s_e/\hbar$, where g^* is an effective electron g factor and s_e is the expectation value of the spin. In general, this g^* is band and \mathbf{k} dependent. For the Γ electrons in the lowest conduction band of GaAs, $g^* = -0.44$.²³ The resulting average magnetic moment for band-edge excitation is thus

$$\bar{\mu}_e = \frac{1}{4}g^*\mu_B, \quad (8)$$

and the rate of electron magnetization injection $\dot{M}_{e;\text{inj}}(\mathbf{r}, t)$ in the sample is then

$$\dot{M}_{e;\text{inj}}(\mathbf{r}, t) = \bar{\mu}_e \dot{n}(\mathbf{r}, t). \quad (9)$$

The magnetic moment of a hole is more complicated than that of an electron. The effective magnetic moment of the heavy- and light-hole states can be written in terms of the Luttinger parameter κ^L .^{6,24} In optical orientation, with σ^+ polarized light, the $m_{j_h} = +\frac{3}{2}$ and $m_{j_h} = +\frac{1}{2}$ hole states are initially populated in a 3:1 ratio. The heavy-hole state has a magnetic moment of $3\kappa^L\mu_B$ and the light-hole state has a magnetic moment of $\kappa^L\mu_B$.²⁵ The mean magnetic moment of the injected holes is then $\bar{\mu}_h = [3(3\kappa^L\mu_B) + 1(\kappa^L\mu_B)]/(3+1)$ or

$$\bar{\mu}_h = \frac{5}{2}\kappa^L\mu_B, \quad (10)$$

and the rate of injected hole magnetization density is

$$\dot{M}_{h;\text{inj}}(\mathbf{r}, t) = \bar{\mu}_h \dot{n}(\mathbf{r}, t). \quad (11)$$

The band-edge value of κ^L is well known for various semiconductors. In bulk GaAs, it is 1.2 at low temperatures.²⁶ The ratio of the mean hole magnetic moment to the mean electron magnetic moment $\bar{\mu}_h/\bar{\mu}_e$ is approximately -27 and indicates that the injected hole magnetization density is an order of magnitude larger than the injected electron magnetization density and with opposite polarity.

However, at energies near the band edge, magnetic properties, such as the g^* factor, can significantly vary from the band-edge result. The above discussion focused on band-edge values. To explore the extent that the phenomenological result above holds at experimentally relevant energies above the band edge, we have evaluated the magnetization-

injection rate by using a microscopic model. From Fermi's golden rule, we can derive the microscopic expression for the magnetization-injection rate for electrons $\dot{M}_{e;\text{inj}}^a$ or holes $\dot{M}_{h;\text{inj}}^a$. We obtain

$$\dot{M}_{e(h);\text{inj}}^a(\mathbf{r}, t) = \lambda_{e(h)}^{abc}(\omega_0)E_{\text{env}}^{b*}(\mathbf{r}, t)E_{\text{env}}^c(\mathbf{r}, t) + \text{c.c.}, \quad (12)$$

where λ_e^{abc} and λ_h^{abc} are optical susceptibility pseudotensors, which are given by

$$\lambda_e^{abc}(\omega) = \frac{2\pi e^2}{\hbar^2} \sum'_{c,v,c'} \int \frac{d^3k}{8\pi^3} \mu_{cc'}^a(\mathbf{k}) \times r_{vc}^b(\mathbf{k})r_{cv}^c(\mathbf{k})\delta[\omega_{cv}(\mathbf{k}) - \omega], \quad (13)$$

and

$$\lambda_h^{abc}(\omega) = -\frac{2\pi e^2}{\hbar^2} \sum'_{c,v,v'} \int \frac{d^3k}{8\pi^3} \mu_{vv'}^a(\mathbf{k}) \times r_{vc}^b(\mathbf{k})r_{cv}^c(\mathbf{k})\delta[\omega_{cv}(\mathbf{k}) - \omega], \quad (14)$$

where in the right-hand side of the equation of λ_h^{abc} for holes, $-\mu_{vv'}^a$ replaces $\mu_{cc'}^a$ in the expression of λ_e^{ab} for electrons. The prime in the summation indicates that one should sum over the degenerate conduction states c and c' when calculating λ_e^{abc} (degenerate valence states v and v' when calculating λ_h^{abc}). For semiconductors in which the bands are spin split by a small energy, coherences can be excited. These can be included in calculations of this type as explained by Bhat *et al.*¹⁹ and Nastos *et al.*²² By using the Brillouin zone symmetry properties of the energy bands and matrix elements, it is found that λ^{abc} is a purely imaginary number.

In GaAs, the only nonzero components of λ^{abc} are

$$\lambda^{xyz} = -\lambda^{xzy} = \lambda^{yzx} = -\lambda^{yxz} = \lambda^{zyx} = -\lambda^{zxy}. \quad (15)$$

It is straightforward to show that a consequence of Eq. (15) is that the injected magnetization lies along the direction of the laser beam propagation. With σ^+ light (a complex field amplitude proportional to $\hat{x} + i\hat{y}$), the average magnetic moment per injected electron (or hole) $\bar{\mu}_{e(h)}^z$ is given by

$$\bar{\mu}_{e(h)}^z(\omega) = \frac{\dot{M}_{e(h);\text{inj}}^z(\mathbf{r}, t)}{\dot{n}(\mathbf{r}, t)} = \frac{\lambda_{e(h)}^{zyx}(\omega)}{\xi^{xx}(\omega)}. \quad (16)$$

Surprisingly, it does not seem that there exists an electronic structure calculation that yields band-edge values (at a photon energy of 1.519 eV) of both $\bar{\mu}_e^z(\omega)$ and $\bar{\mu}_h^z(\omega)$ that agree with the accepted experimental values. *Ab initio* calculations, which are based on the local density approximation, fail to give the correct g^* factor for GaAs. This is undoubtedly related to the failure of these calculations in accurately reproducing the band gap and the effective masses. However, even the $\mathbf{k} \cdot \mathbf{p}$ band models, which use empirically determined parameters, are unable to accurately reproduce the band-edge values. For example, the 14-band (five level) model of Hermann and Weisbuch,²⁷ or of Pfeffer and Zawadzki,²⁸ gives reasonably accurate results for the electron magnetic moment, and thus g^* , but they do not give accurate results for the magnetic Luttinger parameter κ^L or hole magnetic mo-

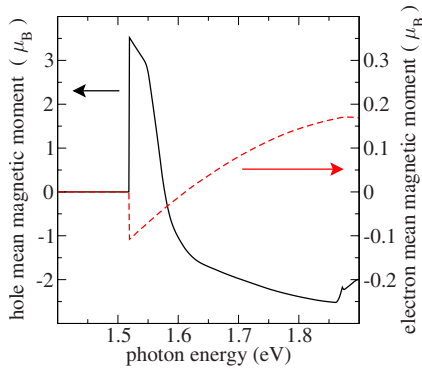


FIG. 2. (Color online) The mean injection electron and hole magnetic moments in GaAs under optical orientation. The hole magnetic moment is typically an order of magnitude larger than the electron magnetic moment. The effective g^* factor for the electrons and the magnetic Luttinger parameter κ^L can be backed out of the figure as described in the text. The change in slope of the hole mean magnetic moment at 1.55 eV is due to the separating of the heavy-hole and light-hole bands.

ments without the use of extra parameters to simulate remote band effects. Moreover, while the 30-band (eight level) model of Richard *et al.*²⁹ gives a value of κ^L close to the experimental result, it gives a very poor g^* factor. Even the refinements to this 30-band model by Fraj *et al.*³⁰ do not give sufficiently accurate results for both the conduction and valence bands.

In a first attempt to understand how the injected magnetization varies away from the band edge, we want a calculation that gives the correct results at the band edge. In the absence of any models that give good-band edge results for both electrons and holes, we adopt the 14-band model of Hermann and Weisbuch²⁷ to calculate the injected magnetic moment per electron and use the 30-band model of Richard *et al.*²⁹ for the holes. The computational details of the calculations follow the spin-injection calculations of Nastos *et al.*,²² and we refer the reader there for details.

In Fig. 2, we plot these magnetic moments as a function of laser photon energy $\hbar\omega$. From the turn-on values at the band edge, g^* and κ^L can be easily backed out by using Eqs. (8) and (10). An important feature shown in Fig. 2 is that the magnetic moments significantly vary near the band edge. Even at 50 meV above the band edge, the injected magnetic moments of both electrons and holes fall to about half their band-edge values. It is important to distinguish the magnetization from the spin. In spin injection in GaAs, it is well established that the band-edge value for the spin polarization of 50% only becomes significantly weaker at excitation energies near the split-off band (about 340 meV above the band edge in GaAs).²²

B. Terahertz radiation from ultrafast magnetization

Terahertz radiation from optically excited electric currents in unbiased semiconductors has been the subject of much recent study. There are many physical effects that lead to terahertz generation.^{31–35} In noncentrosymmetric semiconductors, bulk optical rectification is the dominant source of

terahertz radiation arising from below-band-gap excitation because of the large interaction length. Above the band gap, absorption diminishes the volume of crystal that can contribute to optical rectification, but other effects occur that generate terahertz radiation.

Above-band-gap effects, such as the photo-Dember effect or surface electric field induced optical rectification can induce a strong current, but these currents are typically normal to the surface and so do not radiate terahertz in the normal direction.^{34,36–38} Usual detection schemes for these effects measure terahertz radiation propagating away from the surface normal.

Another class of above-band-gap effects producing terahertz are the photocurrent effects: injection and shift current. The injection current^{17,39} (or circular photogalvanic effect¹⁸) is understood as a $\dot{J}(t)$ that appears in a semiconductor proportional to the laser intensity. However, it vanishes for cubic crystals, and so we do not consider further. The shift current^{35,40,41} (or photogalvanic effect) exists in the zincblende semiconductors and it is understood as a $\dot{P}(t)$ proportional to the laser intensity. It is due to a microscopic shift in the center of charge as carriers are promoted from the valence to the conduction band. For a suitable choice of surface, such as (110) in GaAs, shift currents are excited parallel to the surface plane and so strongly radiate along the surface normal.

The shift current is proportional to the carrier injection rate,

$$\dot{P}_{inj}(\mathbf{r},t) = p\dot{n}(\mathbf{r},t), \quad (17)$$

where $p=ed$ is the average injected dipole moment per carrier. Here, $e=-|e|$ is the electron charge and the displacement d is on the order of a Bohr radius a_B ; for GaAs under excitation with linear polarized light along [110], this distance d is very close to the GaAs bond length, $d=2.54a_B$.²¹ Any back current associated with recombination would occur on a time scale of hundreds of picoseconds and would not lead to radiation in the terahertz regime, so for the shift-current polarization source, we have

$$\dot{P}(\mathbf{r},t) = \dot{P}_{inj}(\mathbf{r},t). \quad (18)$$

In an optical susceptibility formalism, the shift current can be expressed in a form similar to the magnetization injection [Eq. (12)],^{21,42}

$$\dot{P}_{inj}^a(\mathbf{r},t) = \sigma^{abc}(\omega_0)E_{env}^{b*}(\mathbf{r},t)E_{env}^c(\mathbf{r},t) + c.c., \quad (19)$$

where σ^{abc} is a third-rank susceptibility tensor. Unlike the pseudotensor $\lambda_{e(h)}^{abc}$, which describes the magnetization injection and is antisymmetric in its last two indices, the tensor σ^{abc} is symmetric in its last two indices. For GaAs, the non-zero components are

$$\sigma^{xyz} = \sigma^{xzy} = \sigma^{yxz} = \sigma^{yzx} = \sigma^{zxy} = \sigma^{zyx}. \quad (20)$$

It is useful to briefly discuss the implications of the symmetry in Eq. (20) for the case of shift-current excitation in a (110) oriented GaAs surface. For a laser normally incident on a (110) surface, the shift current vanishes by symmetry

for circularly polarized excitation, but it exists for linearly polarized excitation. Moreover, in this case, the shift current is directed in the plane of the surface. Detection of the shift current from linearly polarized light, which is normally incident on (110) GaAs, has been reported by Côté *et al.*³⁵

For non-normal incidence, however, the situation is more complicated and the shift current does not identically vanish for circularly polarized excitation. In this case, there can be a shift current excited in the sample, but when it exists, it is the same for both left- and right-circularly polarized excitations. This is in contrast to the magnetization injection. The pseudotensor symmetries of Eq. (15) dictate that the magnetization points in the opposite directions for left- and right-circularly polarized light.

To estimate the field strength of the terahertz radiation from ultrafast magnetization, we compare it to that arising from the shift current. There are three reasons for making this comparison. First, both the shift current and magnetization injection involve a Maxwell source appearing in the crystal at a constant rate, which allows the comparison to more directly focus on the magnitude of the injected sources and less on their geometrical distribution and temporal profile. The second reason is that the theoretical comparison easily translates into an experimental comparison: With linearly polarized light, only a shift current appears, while with circularly polarized light, magnetization injection also occurs. The final reason is that, for above-band-gap excitation with linearly polarized light, the shift current is believed to be the dominant source of normally emitted terahertz radiation.^{35,40,41}

Before we discuss the realistic scenario of carriers in a semiconductor, it is instructive to consider the case of a free electron in vacuum. The magnetic dipole radiation from flipping the spin of an electron can be directly compared to the electric-dipole radiation from accelerating an electron through a microscopic distance. The change in magnetic moment Δm , under a spin reversal, is $\Delta m = g\mu_B$. The change in electric dipole Δp that is induced by a translation of 1 Bohr is $\Delta p = ea_B$. Assuming that the temporal profiles of these two radiation sources are the same and neglecting the differences in orientation of the radiation patterns, the peak radiation from the magnetization source can be easily compared to the peak radiation from the polarization source by directly comparing the Maxwell sources.⁴³ The radiation from the magnetization source is a factor

$$\frac{\Delta m}{\Delta p} = \frac{g\mu_B}{ea_B} = g\alpha \quad (21)$$

smaller than that from the polarization, where α is the fine-structure constant. For this example of a single electron magnetization source in free space, we see that the magnetic radiation is roughly 70 times smaller than the electric-dipole radiation. A factor of 70, while large, does not preclude a measurement of the terahertz since it is above the signal-to-noise ratio typically encountered in terahertz measurements. However, we must first address the issues that arise when considering carriers in a semiconductor. We require a realistic model for the time dependence of the magnetization source from optical orientation and of the polarization from

the shift current, as well as a procedure for comparing the far-field radiation from these two effects.

Turning to the magnetization source, the total magnetization density $M(\mathbf{r}, t)$ is given by the sum of the hole and electron contributions, $M(\mathbf{r}, t) = M_e(\mathbf{r}, t) + M_h(\mathbf{r}, t)$. Since the lifetime of the injected electron spins is known to be on the order of many picoseconds,² their decay will not contribute to the terahertz radiation and so

$$\dot{M}_e(\mathbf{r}, t) \approx \dot{M}_{e;\text{inj}}(\mathbf{r}, t). \quad (22)$$

However, the lifetime τ_h of the hole spins is in the subpicosecond regime. Assuming that the magnetization decays with the spin, the hole magnetization follows

$$\dot{M}_h(\mathbf{r}, t) = \dot{M}_{h;\text{inj}}(\mathbf{r}, t) - \frac{M_h(\mathbf{r}, t)}{\tau_h}. \quad (23)$$

As accounted for in Eq. (23), the decay reduces the peak magnetization from what it would be if there was no decay.

The far-field radiation from this source will depend on the orientation of the magnetization density in the sample. For excitation with a normally incident laser, the magnetization density will be polarized normal to the surface. Such an orientation does not radiate normal to the surface, where detectors are commonly placed in terahertz detection schemes. To produce significant radiation propagating normal to the surface, the magnetization density must have a component parallel to the plane of the surface, which can be achieved through non-normal incidence. We will discuss the experimental implications of non-normal incidence below, but first we will consider the far-field terahertz radiation from the component of the magnetization source that would be parallel to surface.

We use the notation of Sipe⁴⁴ and write the electric field of the normally emitted terahertz radiation as

$$\mathcal{E}(\mathbf{r}, t) = \int \frac{d\Omega}{2\pi} \int \frac{d\boldsymbol{\kappa}}{(2\pi)^2} \mathcal{E}(\boldsymbol{\kappa}, z, \Omega) e^{i\boldsymbol{\kappa}\cdot\mathbf{R}} e^{-i\Omega t}, \quad (24)$$

where $\mathbf{R}=(x, y)$ lies in the plane parallel to the crystal surface and $\boldsymbol{\kappa}=(\kappa_x, \kappa_y)$. We use a calligraphic $\mathcal{E}(\mathbf{r}, t)$ for the terahertz field to distinguish it from the $\mathbf{E}(t)$ used for the optical field, and we use Ω to distinguish the frequency of the emitted terahertz pulse from the optical frequency ω .

The solution to the Maxwell equations is given by a set of Green's functions. We concentrate on the result for the electric field, and for the radiation emitted from a magnetization, we have

$$\mathcal{E}(\boldsymbol{\kappa}, z, \Omega) = \int dz' \mathbf{G}_{\text{EM}}(\boldsymbol{\kappa}, z - z', \Omega) \cdot \mathbf{M}(\boldsymbol{\kappa}, z', \Omega), \quad (25)$$

where $\mathbf{M}(\boldsymbol{\kappa}, z', \Omega)$ are the Fourier components of the magnetization defined analogous to Eq. (24) and $\mathbf{G}_{\text{EM}}(\boldsymbol{\kappa}, z, \Omega)$ is the planar Green's function.⁴⁴ Similarly, for the polarization source of the shift current, the emitted radiation is given by

$$\mathcal{E}(\boldsymbol{\kappa}, z, \Omega) = \int dz' \mathbf{G}_{\text{EP}}(\boldsymbol{\kappa}, z - z', \Omega) \cdot \mathbf{P}(\boldsymbol{\kappa}, z', \Omega), \quad (26)$$

where $\mathbf{P}(\boldsymbol{\kappa}, z', \Omega)$ are the Fourier components of the polarization density and $\mathbf{G}_{\text{EP}}(\boldsymbol{\kappa}, z, \Omega)$ as the appropriate Green's function.

To obtain the far-field radiation in the normal direction for $z > 0$, we let $r \rightarrow \infty$ and find that the asymptotic form is determined by a neighborhood of $\boldsymbol{\kappa}$ around $\boldsymbol{\kappa} = 0$. Assuming that the magnetization source is polarized along $\hat{\mathbf{x}}$, we find that the electric field $\mathcal{E}(z, t)$ from the source is polarized along $\hat{\mathbf{y}}$ and its magnitude is given by

$$\mathcal{E}(z, t) = \frac{1}{z} \mathcal{F}_M(t - z/c), \quad (27)$$

where the Fourier components of $\mathcal{F}_M(t)$ are given by

$$\mathcal{F}_M(\Omega) = -\frac{\Omega^2}{c^2} \frac{2}{n+1} n M_+(\Omega), \quad (28)$$

and where M_+ is given by

$$M_+(\Omega) = \int_{-L}^0 dz' e^{-i\Omega n z'/c} M(0, z', \Omega). \quad (29)$$

The phase $-i\Omega n z'/c$ accounts for path lengths experienced by radiation emitted at different depths in the sample. In Eq. (28), the index of refraction n appearing in the denominator comes from the Green's function \mathbf{G}_{EM} and the factor Ω^2 appears because the far-field radiation depends on the second derivative of $M(t)$.

For the far-field normal radiation from a polarization source, that is polarized along $\hat{\mathbf{x}}$, we find that the terahertz radiation is $\hat{\mathbf{x}}$ polarized and that

$$\mathcal{E}(t) = \frac{1}{z} \mathcal{F}_P(t - z/c), \quad (30)$$

where the Fourier components are given by

$$\mathcal{F}_P(\Omega) = \frac{\Omega^2}{c^2} \frac{2}{n+1} P_+(\Omega), \quad (31)$$

where $P_+(\Omega)$ is given by

$$P_+(\Omega) = \int_{-L}^0 dz' e^{-i\Omega n z'/c} P(0, z', \Omega). \quad (32)$$

The far-field terahertz radiation from the shift current has been detected in other studies. We will use this to estimate a baseline signal-to-noise ratio needed to measure terahertz radiation from the magnetization source. We will compare the magnetization source, which is maximized for circular polarizations, to the shift-current source, which is maximized for linear polarized light.

Since the magnetization density of the electrons is much smaller than the holes, a simple estimate of the radiation from the magnetization can be made by comparing only the hole magnetization source to the polarization induced by the shift current. We will compare just the Fourier spectra \mathcal{F}_M and \mathcal{F}_P . For the forms [Eqs. (18) and (23)] assumed for our source terms, we find

$$\frac{\mathcal{F}_M(\Omega)}{\mathcal{F}_P(\Omega)} = \frac{i\Omega\tau_h n \dot{M}_{h;\text{inj}}(\Omega)}{i\Omega\tau_h - 1 \dot{P}_{\text{inj}}(\Omega)}. \quad (33)$$

Since $\Delta\Omega$ is on the order of 10 THz, we have $\Omega\tau_h \approx 1$, and by using Eqs. (11) and (17),

$$\left| \frac{\mathcal{F}_M(\Delta\Omega)}{\mathcal{F}_P(\Delta\Omega)} \right| = (0.7)n \frac{\bar{\mu}_h}{p} = (2.8) \frac{\kappa^L}{(d/a_B)} \alpha, \quad (34)$$

where α is the fine-structure constant. With parameters for GaAs ($n=3.2$, $\kappa^L=1.2$, and $d=2.54a_B$), we have $|\frac{\mathcal{F}_M(\Delta\Omega)}{\mathcal{F}_P(\Delta\Omega)}| \approx 0.01$. That is, the ratio of the magnetization to polarization signal is about 1%. This is comparable to the simple estimate [Eq. (21)] of that ratio for a single electron, although in the calculation here we have included effects associated with the temporal behavior of the sources, the transmission of the generated terahertz through the surface, the large magnetic moment associated with the hole, and the actual shift distance associated with absorption. Of course, the terahertz radiation from the ultrafast magnetization needs not to be extracted from a signal containing the much stronger terahertz radiation from the shift current. There are crystal orientations for which the ultrafast magnetization is only produced when the incident laser field is circularly polarized, and the shift current is only produced when the incident laser field is linearly polarized. The requirement to detect a signal approximately 100 times weaker than that from the shift current is experimentally challenging but not impossible. This is because the terahertz field amplitude, rather than the intensity, is experimentally measured. If the intensity were measured, the signal from the magnetization effect would be reduced from that of the shift current by a factor of $[\mathcal{F}_M(\Delta\Omega)/\mathcal{F}_P(\Delta\Omega)]^2$.

III. EXPERIMENT

We now turn to our experimental search for the terahertz signal from the magnetization source. Figures 3(a) and 3(b) illustrate our experimental setup for observing the transient terahertz radiation. An 80 MHz Ti:sapphire oscillator delivers 1 nJ, 100 fs pulses at 800 nm. For this wavelength, the injected kinetic energies of heavy holes and light holes are 3.6 and 9.5 meV, respectively. This is much less than the 340 meV needed to excite holes in the spin-orbit split-off band. The pulses are split into a pump beam for sample excitation and a probe beam to sample terahertz radiation via electro-optic sampling.

The pump beam is incident onto a 100 μm thick (110) oriented GaAs sample. We define $\hat{\mathbf{z}}$ to be the surface normal of the sample. The incident laser beam lies in the xz plane. The direction $\hat{\mathbf{y}}$ points out of the page in Fig. 3(b) and corresponds to usual $\hat{\mathbf{s}}$ vector commonly defined for non-normal incidence. The [001] crystal axis lies along the plane of the sample surface (xy plane). We denote the angle between the [001] crystal axis and $\hat{\mathbf{y}}$ by γ . We set $\gamma=1.2^\circ$, so that for linear polarizations we have a small but detectable terahertz signal, which we model as being from the shift current.⁴⁰

The pump beam polarization is controlled by half- and quarter-wave plates (HWP and QWP) and a photoelastic

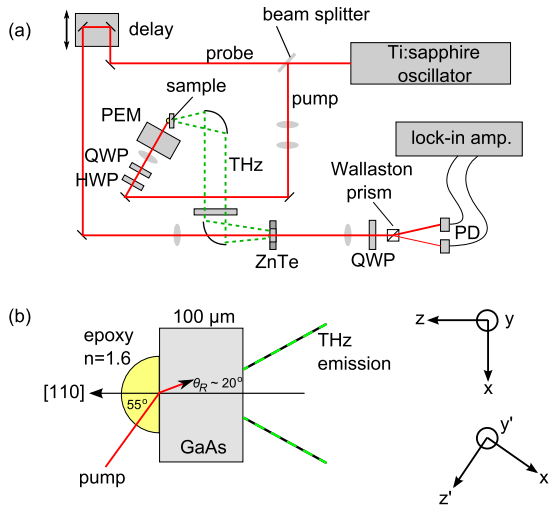


FIG. 3. (Color online) (a) Experimental setup. (b) Top view of sample with epoxy hemisphere. PEM: photoelastic modulator; HWP: half wave-plate; QWP: quarter-wave plate; and PD: photodiode.

modulator (PEM), as in Fig. 3(a). The HWP is oriented to provide light linearly polarized 45° from \hat{y} and fixed. The QWP is used to alternate between circular and linear excitations. We introduce the angle β , which is defined as the angle between the QWP fast axis and \hat{y} , and rotate the QWP to sweep β from 0° to 180° . The PEM operates in quarter-wave mode and modulates the polarization state at a frequency of 42 kHz. Lock-in detection and amplification let us measure the difference in terahertz signals from two polarization states, which we call state 1 and state 2. In state 1, the PEM behaves like a QWP with its fast axis at $\pi/2$ and in state 2, it behaves like a QWP with its fast axis at 0° .

To describe the effect of the optical elements, we introduce the primed coordinate system $\{\hat{x}', \hat{y}', \hat{z}'\}$, as shown in Fig. 3(b). The incident laser beam travels along $-\hat{z}'$. After the QWP, the laser beam polarization is given by

$$\begin{aligned} \begin{bmatrix} E_{x'} \\ E_{y'} \end{bmatrix} &= \frac{E_0}{\sqrt{2}} \begin{bmatrix} \cos \beta (\sin \beta + \cos \beta) + i \sin \beta (\sin \beta - \cos \beta) \\ \sin \beta (\sin \beta + \cos \beta) + i \cos \beta (\cos \beta - \sin \beta) \end{bmatrix}. \end{aligned} \quad (35)$$

The PEM then acts like another QWP. In what we call state 1, the beam polarization after the PEM is

$$\begin{aligned} \begin{bmatrix} E_{x'} \\ E_{y'} \end{bmatrix}_{\text{state1}} &= \frac{E_0}{\sqrt{2}} \begin{bmatrix} \sin \beta (\cos \beta - \sin \beta) + i \cos \beta (\sin \beta + \cos \beta) \\ \sin \beta (\cos \beta + \sin \beta) + i \cos \beta (\cos \beta - \sin \beta) \end{bmatrix}. \end{aligned} \quad (36)$$

In what we call state 2, the beam polarization after the PEM is

$$\begin{aligned} \begin{bmatrix} E_{x'} \\ E_{y'} \end{bmatrix}_{\text{state2}} &= \frac{E_0}{\sqrt{2}} \begin{bmatrix} \cos \beta (\cos \beta + \sin \beta) + i \sin \beta (\sin \beta - \cos \beta) \\ \cos \beta (\sin \beta - \cos \beta) + i \sin \beta (\cos \beta + \sin \beta) \end{bmatrix}. \end{aligned} \quad (37)$$

We use an angle of incidence of 55° , with excitation through an epoxy hemisphere, with index of 1.6, to give an angle of refraction θ_R inside the GaAs sample of about 20° . The laser has a spot diameter of $25 \mu\text{m}$, which produces a peak incident intensity of 500 MW/cm^2 and a carrier density of $2 \times 10^{18} \text{ cm}^{-3}$ over an absorption depth of about $1 \mu\text{m}$. Since the total magnetization or electric polarization is determined by the total number of carriers excited, and not their density, there is no premium associated with beam focusing.

The terahertz radiation emitted along the surface normal, in the forward direction, is collected with an $f=50 \text{ mm}$, 90° off-axis parabolic, and focused with the same type of mirror onto a $500 \mu\text{m}$ thick (110) ZnTe electro-optic sampling crystal. The 800 nm probe pulse is spatially overlapped with the terahertz field inside the ZnTe crystal and temporally scanned by adjusting the delay.

The non-normal incidence introduces a minor complication. In addition to a shift current that exists from linearly polarized excitation, because of the non-normal incidence, a shift current is also excited from circularly polarized excitation. To identify the contribution to the terahertz signal from the injected magnetization, we rely on the different symmetries of the pseudotensor λ^{abc} [Eq. (15)] and the tensor σ^{abc} [Eq. (20)]. Unlike the magnetization, which reverses sign when the light polarization is changed from right to left circular, the shift current is the same for both right- and left-circularly polarized excitations. Thus, the contribution to our detected terahertz signal from this extraneous shift-current signal, and any other χ_2^{abc} electric susceptibility effect satisfying the symmetries in Eq. (20), is eliminated by using the photoelastic modulator together with the lock-in detection.

A simple coordinate rotation can be used to convert the polarization vectors in Eqs. (36) and (37) from $\{\hat{x}', \hat{y}', \hat{z}'\}$ to $\{\hat{x}, \hat{y}, \hat{z}\}$ [see Fig. 3(b)]. The material polarization and magnetization from the shift current and magnetization injection can be calculated by using Eq. (19) and (12), respectively. After a rotation back to the primed coordinate system, one component of each the polarization and magnetization vectors is taken as a measure of the radiant terahertz emission detected. This is because the dipole radiation $E_{\text{shift}}^{\text{THz}}$ from the shift-current source is polarized along the dipole direction, and the radiation from the magnetization source $E_{\text{mag}}^{\text{THz}}$ is polarized orthogonal to the magnetization direction. This can be summarized as $E_{\text{shift}}^{\text{THz}} \sim P_{\text{inj};\text{shift}}^y$ and $E_{\text{mag}}^{\text{THz}} \sim M_{\text{inj};\text{mag}}^x$.

The terahertz radiation signal we measure, ΔE_{THz} , is the difference in terahertz field \hat{y} components of the two polarization states we are modulating between, that is,

$$\Delta E_{\text{THz}} = E_{\text{THz}; \text{state 1}} - E_{\text{THz}; \text{state 2}}. \quad (38)$$

After including the transmission through the sample interface and applying Eqs. (11), (12), (17), and (19), for the radiation from the shift current, we obtain

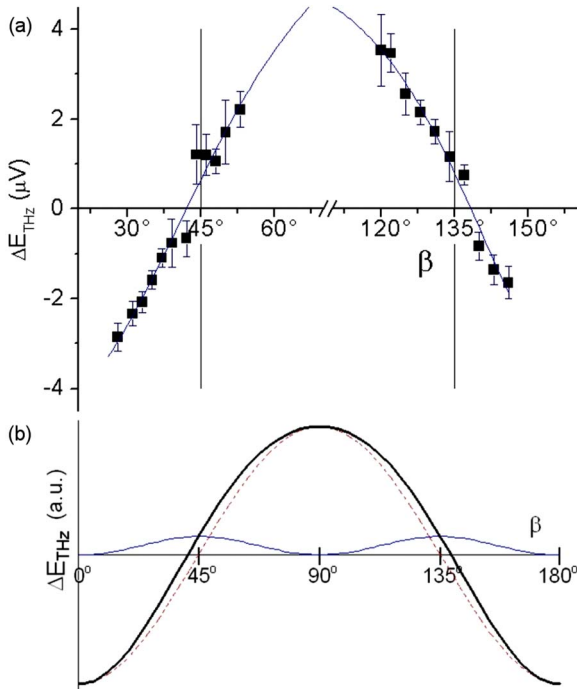


FIG. 4. (Color online) (a) Experimental results (points) with Fourier-series fit (curve). (b) Simulation of terahertz signal vs QWP angle β . Red dashed line: shift-current signal; blue thin line: magnetization signal; and black thick line: total signal.

$$\Delta E_{\text{THz}}^{\text{shift}} = Ced \cos(\theta_R)(2 \sin \gamma - 3 \sin^3 \gamma)\cos(2\beta), \quad (39)$$

and from the ultrafast magnetization, we obtain

$$\Delta E_{\text{THz}}^{\text{mag}} = Cn\mu_{\text{eff}} \sin(\theta_R)\sin^2(2\beta), \quad (40)$$

where the constant C depends on the width of the pulse and is proportional to the product of the Fresnel transmission coefficients for s - and p -polarized electric fields across the epoxy-air interface. This dependency is not obvious but results from the cancellation of terms in Eq. (38). The effective magnetic moment μ_{eff} describes the sum of electron and hole magnetic moments, but we expect it to be dominated by the hole term, and so from Eq. (34), we take $\mu_{\text{eff}}=(0.7)\bar{\mu}_h$. It is evident from the β dependence of Eqs. (39) and (40) that the shift-current signal is maximized when $\beta=0^\circ$ and minimized when $\beta=45^\circ$; the magnetization signal is maximized when $\beta=45^\circ$ and minimized when $\beta=0^\circ$. When $\cos(2\beta)=0$, the incident light polarization is modulating between $+45^\circ$ and -45° linear, and when $\sin(2\beta)=0$, it is modulating between right- and left-circularly polarized states.

Figure 4(a) shows the results from experimental measurements of the terahertz field strength as a function of β . The terahertz field strength is defined as the peak-to-peak value of the observed terahertz trace, although several other definitions of signal strength were used and each resulted in a similar pattern as a function of β . The deviation of the sinusoidal pattern created by the shift current is attributed to the signal from the magnetization source. The zero crossings of the Fourier-series fit to the data of Fig. 4(a) are separated by more than 90° indicating the presence of an additional tera-

hertz source with a β dependence, as shown in Fig. 4(b). The amplitudes recorded at maximum, $\beta=90^\circ$, and minimum, $\beta=0^\circ$, sum up to nearly zero ($0.05 \pm 0.14 \mu\text{V}$). A vertical offset of at least $1 \mu\text{V}$ would have been required to cause the zero crossing deviation as present in the data. The experiment yields that the relative strengths of the magnetization and shift-current sources have a ratio 0.017, which is of the same order of magnitude as the theoretical estimate. Figure 4(b) illustrates the expected variation in the terahertz field strength from the shift and magnetization sources, taking the ratio of the source strengths to be 0.017.

Possible sources of systematic error must be mentioned. The terahertz radiation from optical rectification above the band gap was neglected, since it is small relative to that from the shift current and shares the same symmetry dependence. The possibility of terahertz radiation from surface sources is being investigated. Terahertz radiation related to the Dember fields have no dependence on crystal orientation or pump polarization. Despite the assumption of the shift current as the only significant competing terahertz source, this initial effort shows that a terahertz signal on the order of that predicted from the magnetization in bulk GaAs can and has been measured. Other sources of experimental error have been investigated. For example, we have examined angular offset errors to the initial pump or probe polarization, the polarization optics (HWP, QWP, and PEM), and the electro-optic detection system. All of such errors produce either a uniform shift of the β plot right or left or a small scaling factor. None can be found to exhibit the same dependency on β as the magnetization source.

IV. CONCLUSION

In conclusion, we have theoretically investigated the magnetic properties of electrons and holes that are created by optical excitation with above-band-gap circularly polarized light in semiconductors. We have derived expressions for the magnetization-injection rates of electrons and holes within the independent particle picture and have calculated them for GaAs with $\mathbf{k}\cdot\mathbf{p}$ band models. We find that the injected hole magnetic moments are generally an order of magnitude larger than those of the injected electrons.

We have investigated the possibility of measuring the terahertz radiation from this transient ultrafast magnetization of holes in GaAs. We have theoretically shown that the terahertz radiation from circularly polarized excitation is large enough to be detected, and we have presented initial experiments in search of this radiation. For a fixed angle of incidence, we have measured the normally emitted terahertz radiation as a function of modulated elliptical polarization of the incident beam. By using a rough measure for the strength of the terahertz field, we have found it to fit within a factor of 2, which would be expected if the signal was comprised of only a magnetization and shift-current signal. While the results are preliminary, we find them encouraging.

Future experiments investigating the terahertz radiation can improve on what we have done here by taking a more systematic approach to the experimental parameters. For example, measuring the polarization of the terahertz as a func-

tion of emitted angle would provide a stronger signature for a magnetization source. Additionally, the terahertz generation depends on the injection rate of magnetized carriers, and so by using a shorter pulse increases the injection rate and the terahertz signal. The terahertz signal from the injected magnetization could also be increased by using materials with a larger Luttinger parameter κ^L or g factor. Materials with g factors near 50, such as InSb, have been reported.⁴⁵ Finally, the actual profiles of the emitted terahertz fields, which we have not discussed but which can easily be determined

through an extension of the analysis in Sec. II B, could be analyzed in an attempt to carefully back out the temporal profile of the sources.

ACKNOWLEDGMENTS

We thank J. Prineas, C. Pryor, A. Bristow, M. Betz, and J. Rioux for useful discussions. Preliminary experimental work by Q. H. Wang is also acknowledged. This work is supported by NSERC, Photonics Research Ontario, and DARPA SpinS.

*Present address: Institute for Solid State Physics, University of Hannover, Appelstrasse 2, 30167 Hannover, Germany.

- ¹M. I. Dyakanov and V. I. Perel, in *Optical Orientation*, edited by F. Meier and B. P. Zakharchenya (Elsevier, Amsterdam, 1984), Chap. 2, pp. 11–71.
- ²I. Žutić, J. Fabian, and S. D. Sarma, *Rev. Mod. Phys.* **76**, 323 (2004).
- ³M. Oestreich *et al.*, *Semicond. Sci. Technol.* **17**, 285 (2002).
- ⁴D. D. Awschalom and J. M. Kikkawa, *Phys. Today* **52**(6), 33 (1999).
- ⁵D. J. Hilton and C. L. Tang, *Phys. Rev. Lett.* **89**, 146601 (2002).
- ⁶J. M. Luttinger, *Phys. Rev.* **102**, 1030 (1956).
- ⁷L. M. Roth, *Phys. Rev.* **118**, 1534 (1960).
- ⁸J. P. van der Ziel, P. S. Pershan, and L. D. Malmstrom, *Phys. Rev. Lett.* **15**, 190 (1965).
- ⁹P. S. Pershan, J. P. van der Ziel, and L. D. Malmstrom, *Phys. Rev.* **143**, 574 (1966).
- ¹⁰L. P. Pitaevskii, *Sov. Phys. JETP* **12**, 1008 (1961).
- ¹¹R. Hertel, *J. Magn. Magn. Mater.* **303**, L1 (2006).
- ¹²S. V. Popov, N. I. Zheludev, and Y. P. Svirko, *Opt. Lett.* **19**, 13 (1994).
- ¹³Y. Kato, R. C. Myers, A. C. Gossard, and D. D. Awschalom, *Nature (London)* **427**, 50 (2004).
- ¹⁴M. Atatüre, J. Dreiser, A. Badolato, and A. Imamoglu, *Nat. Phys.* **3**, 101 (2007).
- ¹⁵S. A. Crooker, D. D. Awschalom, J. J. Baumberg, F. Flack, and N. Samarth, *Phys. Rev. B* **56**, 7574 (1997).
- ¹⁶P. Yu and M. Cardona, *Fundamentals of Semiconductors* (Springer, New York, 1996).
- ¹⁷N. Laman, A. I. Shkrebtii, J. E. Sipe, and H. M. van Driel, *Appl. Phys. Lett.* **75**, 2581 (1999).
- ¹⁸B. I. Sturman and V. M. Fridkin, *The Photovoltaic and Photo-refractive Effects in Noncentrosymmetric Materials* (Gordon and Breach, Philadelphia, 1992).
- ¹⁹R. D. R. Bhat, F. Nastos, A. Najmaie, and J. E. Sipe, *Phys. Rev. Lett.* **94**, 096603 (2005).
- ²⁰R. von Baltz and W. Kraut, *Phys. Rev. B* **23**, 5590 (1981).
- ²¹F. Nastos and J. E. Sipe, *Phys. Rev. B* **74**, 035201 (2006).
- ²²F. Nastos, J. Rioux, M. Strimas-Mackey, B. S. Mendoza, and J. E. Sipe, *Phys. Rev. B* **76**, 205113 (2007).
- ²³C. Weisbuch and C. Hermann, *Phys. Rev. B* **15**, 816 (1977).
- ²⁴A. A. Kiselev, K. W. Kim, and E. Yablonovitch, *Phys. Rev. B*

64, 125303 (2001).

- ²⁵Effective g^* factors for the holes can be introduced, but there is apparently not a unique convention in literature. The relation of the magnetic moment to κ^L is, however, unambiguous.
- ²⁶Q. X. Zhao, P. O. Holtz, A. Pasquarello, B. Monemar, A. C. Ferreira, M. Sundaram, J. L. Merz, and A. C. Gossard, *Phys. Rev. B* **49**, 10794 (1994).
- ²⁷C. Hermann and C. Weisbuch, *Phys. Rev. B* **15**, 823 (1977).
- ²⁸P. Pfeffer and W. Zawadzki, *Phys. Rev. B* **53**, 12813 (1996).
- ²⁹S. Richard, F. Aniel, and G. Fishman, *Phys. Rev. B* **70**, 235204 (2004).
- ³⁰N. Fraj, S. B. Radhia, and K. Boujdaria, *Solid State Commun.* **142**, 342 (2007).
- ³¹K. Wynne and J. J. Carey, *Opt. Commun.* **256**, 400 (2005).
- ³²E. Beaurepaire, G. M. Turner, S. M. Harrel, M. C. Beard, J.-Y. Bigot, and C. A. Schmuttenmaer, *Appl. Phys. Lett.* **84**, 3465 (2004).
- ³³C. A. Schmuttenmaer, *Chem. Rev. (Washington, D.C.)* **104**, 1759 (2004).
- ³⁴M. B. Johnston, D. M. Whittaker, A. Corchia, A. G. Davies, and E. H. Linfield, *Phys. Rev. B* **65**, 165301 (2002).
- ³⁵D. Côté, N. Laman, and H. M. van Driel, *Appl. Phys. Lett.* **80**, 905 (2002).
- ³⁶B. B. Hu, X.-C. Zhang, and D. H. Auston, *Phys. Rev. Lett.* **67**, 2709 (1991).
- ³⁷X. C. Zhang, B. B. Hu, J. T. Darrow, and D. H. Auston, *Appl. Phys. Lett.* **56**, 1011 (1990).
- ³⁸S. L. Chuang, S. Schmitt-Rink, B. I. Greene, P. N. Saeta, and A. F. J. Levi, *Phys. Rev. Lett.* **68**, 102 (1992).
- ³⁹N. Laman, M. Bieler, and H. M. van Driel, *J. Appl. Phys.* **98**, 103507 (2005).
- ⁴⁰R. Adomavičius, G. Molis, A. Krotkus, and V. Sirutkaitis, *Appl. Phys. Lett.* **87**, 261101 (2005).
- ⁴¹M. Bieler, K. Pierz, U. Siegner, and P. Dawson, *Phys. Rev. B* **76**, 161304(R) (2007).
- ⁴²J. E. Sipe and A. I. Shkrebtii, *Phys. Rev. B* **61**, 5337 (2000).
- ⁴³J. D. Jackson, *Classical Electrodynamics*, 3rd ed. (Wiley, New York, 1999).
- ⁴⁴J. E. Sipe, *J. Opt. Soc. Am. B* **4**, 481 (1987).
- ⁴⁵L. M. Roth, B. Lax, and S. Zwerdling, *Phys. Rev.* **114**, 90 (1959).